Diminution of HTLV-1 provirus load by intake of encapsulated green tea extract powder. The HTLV-1 provirus loads in the GT(−) group and GT(+) group at the beginning of the follow-up study were 0.2–200.2 and 0.2–192.0 copies/1000 cells, and the mean and standard deviation were 43.2±52.3 and 33.4±45.9, respectively (Fig. 4, A and B, 0 month). The HTLV-1 provirus load in both groups showed no statistically significant difference (P=0.369). The follow-up observation revealed that GT(−) group subjects above the median value had a wide range of fluctuation in HTLV-1 provirus load during the study period, whereas those below the median value maintained consistently low levels of HTLV-1 provirus load (Fig. 4A, 0–5 months). The GT(+) group showed a lesser fluctuation of HTLV-1 provirus load above the median value after intake of the green tea capsules (Fig. 4B, 0–5 months).

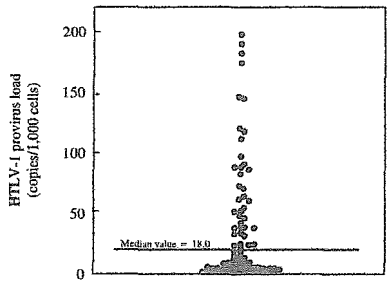

Fig. 3. Individual variation of HTLV-1 provirus load among HTLV-1 carriers. The median value of HTLV-1 provirus load among 83 study subjects was 18.0 copies/1000 cells. Note the skewed distribution, with a wide range of variation and clustering at levels below the median value of HTLV-1 provirus load.

The difference in HTLV-1 provirus load from baseline to each follow-up month between the GT(−) and GT(+) groups was not great, but reached statistical significance at 5 months in the subgroup of higher provirus load (Table 2, P=0.031). No significant difference was observed in the lower provirus load group.

Changing trend of HTLV-1 provirus load over time among HTLV-1 carriers. Among the subgroup of higher provirus load group, a decreasing trend of the HTLV-1 provirus load values was observed in the GT(+) group (regression coefficient (RC)= −0.072, SE=0.430), but not in the GT(−) group (RC=+0.012, SE=0.043), and the difference showed a marginal significance (P=0.077). This trend did not change after adjustment for age (RC of GT(+) and GT(−)=−0.072 and +0.012, respectively), smoking (RC=−0.071, +0.013), and alcohol drinking (RC= −0.072, +0.012).

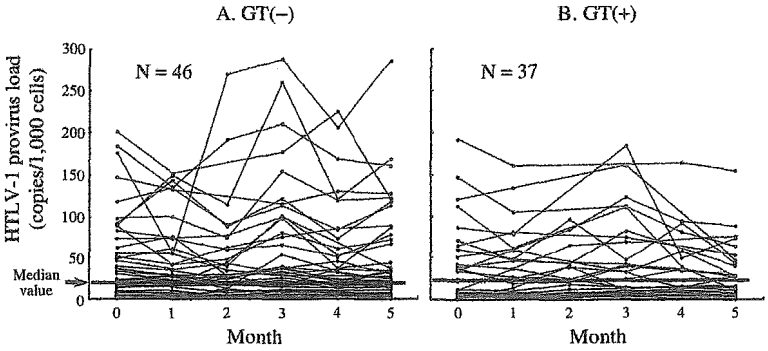

Fig. 4. Change in HTLV-1 provirus load during 5 months follow-up of HTLV-1 carriers with or without administration of green tea powder capsules ("Nanchariki"). (A) GT(−); 46 subjects lived without restriction of their lifestyle as a control group. They were followed up for 5 months by measuring HTLV-1 provirus DNA by duplicate intra-assay using 6 blood samples obtained from each subject. The median value of 18.0 copies/1000 cells was the same as that in Fig. 3. (B) GT(+); 37 subjects received 9 capsules of "Nanchariki" and the HTLV-1 provirus loads were measured by duplicate intra-assay as described above.

Table 2. Comparison of HTLV-1 provirus load difference from baseline to each follow-up month between GT(−) and GT(+) groups

	Number	Values of provirus load					
		Baseline	Difference between baseline and each month				
		0 month	1 month	2 months	3 months	4 months	5 months
		Mean±SD	Mean±SD	Mean±SD	Mean±SD	Mean±SD	Mean±SD
Total							
GT(−)	46	42.1±52.4	−4.1±25.6	−2.5±20.2	11.6±39.0	−2.1±14.4	1.5±27.4
GT(+)	37	32.8±46.3	−2.6±15.4	5.5±14.1	8.7±24.9	−4.9±26.5	−7.8±27.4
P values		—	0.616	0.946	0.364	0.301	0.063
Lower provirus load group[1)]							
GT(−)	20	4.6±5.2	−0.2±1.7	0.4±6.2	0.8±7.0	−0.1±4.1	−0.1±3.0
GT(+)	21	3.8±3.4	1.6±6.5	4.8±10.6	2.0±3.2	2.4±3.5	1.6±3.6
P values		—	0.873	0.892	0.722	0.936	0.936
Higher provirus load group[2)]							
GT(−)	26	72.6±53.2	−7.2±34.0	−4.1±25.0	17.2±47.2	−3.2±17.8	2.7±36.6
GT(+)	16	66.6±49.1	−8.1±21.3	6.6±18.8	15.4±34.3	−12.2±36.7	−20.2±38.7
P values		—	0.46	0.874	0.45	0.169	0.031

Note the statistical significance of the difference of HTLV-1 provirus load at 5 months in the higher load group.
1) The subjects with an HTLV-1 provirus load lower than 18.0 copies/1000 cells at baseline.
2) The subjects with an HTLV-1 provirus load higher than 18.0 copies/1000 cells at baseline.

Discussion

The present study was designed to investigate the *in vivo* effect of green tea on HTLV-1 provirus load by administering green tea powder capsules ("Nanchariki") to HTLV-1 carriers. The real-time PCR quantification of HTLV-1 provirus DNA has an inherent error of 25% in terms of coefficient of variation (CV), as was seen in different inter-assay runs for HTLV-1 provirus load.[26] However, our real-time PCR quantification with duplicate intra-assay reduced the CV to less than 8% (Fig. 2). By virtue of this method, we could perform accurate measurements of HTLV-1 provirus load in peripheral blood lymphocytes of asymptomatic HTLV-1 carriers, revealing a wide range of variation and fluctuation of HTLV-1 provirus load among HTLV-1 carriers (Fig. 3, Fig. 4). Similar findings were documented by the Miyazaki cohort study.[10]

Daily intake of 9 capsules of "Nanchariki" for 5 months diminished the HTLV-1 provirus load in the higher provirus load group. The extent of diminution was not great but the HTLV-1 provirus load showed a consistent diminution over time in the GT(+) group (RC=−0.072). This marginal extent of HTLV-1 diminution can be explained by three possibilities. The first possibility is that the dose of the green tea extract powder used in this study (9 capsules of "Nanchariki") is insufficient for suppression of HTLV-1 carriers' lymphocytes *in vivo*, since the concentration of EGCg in plasma is estimated to be about 0.3 μg/ml,[27] which is far less than the range of 3–27 μg/ml required to inhibit the growth of HTLV-1-infected T-cells *in vitro*.[22] The second is that the majority of the HTLV-1 carriers are females, who may have fewer abnormal lymphocytes in the circulation than males[28,29] and their HTLV-1-infected lymphocytes may be less sensitive to apoptosis induction by green tea components.[22] The third is that individual variation in absorption and metabolism of tea polyphenols[30] may produce heterogeneous responses in diminution of HTLV-1 provirus load, so that it is difficult to obtain a consistent result with statistical significance.

Work on the molecular mechanisms of HTLV-1 suppression by green tea polyphenols has been focused on the transcriptional factors, I-κB/NF-κB.[31] HTLV-1 Tax protein degrades I-κB and activates NF-κB, and then enhances IL-2/IL-2 receptor expression in HTLV-1-infected T-cells.[32] EGCg of green tea polyphenols stabilizes I-κB and abrogates NF-κB activation in keratinocytes.[31] Stabilization of I-κB and abrogation of NF-κB activation may occur in HTLV-1 carrier lymphocytes after intake of green tea capsules. Individuals with a higher provirus load, who are at risk for ATL, may derive particular benefit from green tea drinking because they have increased number of abnormal lymphocytes that are prone to apoptosis.[22,29,33]

"Nanchariki" is made of whole extract of green tea, which contains caffeine and polyphenol compounds. Decaffeinated capsules of green tea extract powder may minimize in the effects on the stomach and bowel movements encountered in the drop-out cases in this study. We have already developed decaffeinated capsules, and a further study is planned.

In conclusion, the present study has demonstrated a diminution of HTLV-1 provirus load in peripheral blood lymphocytes of HTLV-1 carriers taking "Nanchariki" capsules. Further study on the mechanism of suppression of transcriptional factors and induction of apoptosis of HTLV-1-infected lymphocytes by green tea may provide an insight into chemoprevention of other virus-related cancers.

We thank Mrs. Ranko Kawata-Tsurumaru for her secretarial work and Mr. Glenn Forbes for English editing. This study was supported in part by Grants-in-Aid for Scientific Research on Priority Areas for Cancer from the Ministry of Education, Culture, Sports, Science and Technology of Japan (No.12218232 and 12218104) and a Research Fellowship from the Japan Society for the Promotion of Science for Young Scientists.

1. Uchiyama T, Yodoi J, Sagawa K, Takatsuki K, Uchino H. Adult T-cell leukemia: clinical and hematologic features of 16 cases. *Blood* 1977; **50**: 481–92.
2. Hinuma Y, Nagata K, Hanaoka M, Nakai M, Matsumoto T, Kinoshita KI, Shirakawa S, Miyoshi I. Adult T-cell leukemia: antigen in an ATL cell line and detection of antibodies to the antigen in human sera. *Proc Natl Acad Sci USA* 1981; **78**: 6476–80.
3. Osame M, Usuku K, Izumo S, Ijichi N, Amitani H, Igata A, Matsumoto M, Tara M. HTLV-I associated myelopathy, a new clinical entity. *Lancet* 1986; **i**: 1031–2.
4. Gessain A, Barin F, Vernant JC, Gout O, Maurs L, Calender A, de The G. Antibodies to human T-lymphotropic virus type-I in patients with tropical spastic paraparesis. *Lancet* 1985; **ii**: 407–10.
5. Hino S, Katamine S, Miyata H, Tsuji Y, Yamabe T, Miyamoto T. Primary prevention of HTLV-1 in Japan. *Leukemia* 1997; **Suppl 3**: 57–9.
6. Takahashi K, Takezaki T, Oki T, Kawakami K, Yashiki S, Fujiyoshi T, Usuku K, Mueller N, Osame M, Miyata K, Nagata Y, Sonoda S. The Mother-to-Child Transmission Study Group. Inhibitory effect of maternal antibody on mother-to-child transmission of human T-lymphotropic virus type I. *Int J Cancer* 1991; **49**: 673–7.
7. Taylor GP, Tosswill JH, Matutes E, Daenke S, Hall S, Bain BJ, Davis R, Thomas D, Rossor M, Bangham CR, Weber JN. Prospective study of HTLV-I infection in an initially asymptomatic cohort. *J Acquir Immune Defic Syndr* 1999; **22**: 92–100.
8. Hisada M, Okayama A, Shioiri S, Spiegelman DL, Stuver SO, Mueller NE. Risk factors for adult T-cell leukemia among carriers of human T-lymphotropic virus type I. *Blood* 1998; **92**: 3557–61.
9. Manns A, Miley WJ, Wilks RJ, Morgan OS, Hanchard B, Wharfe G, Cranston B, Maloney E, Wells SL, Blattner WA, Waters D. Quantitative proviral DNA and antibody levels in the natural history of HTLV-I infection. *J Infect Dis* 1999; **180**: 1487–93.
10. Okayama A, Stuver SO. Long-term follow-up of HTLV-1 carriers. In: Two decades of adult T-cell leukemia and HTLV-1 research. *Gann Monogr* 2003; **50**: 127–39.
11. Rice-Evans C. Implications of the mechanisms of action of tea polyphenols as antioxidants *in vitro* for chemoprevention in humans. *Proc Soc Exp Biol Med* 1999; **220**: 262–6.
12. Wiseman SA, Balentine DA, Frei B. Antioxidants in tea. *Crit Rev Food Sci Nutr* 1997; **37**: 705–18.
13. Muto S, Yokoi T, Gondo Y, Katsuki M, Shioyama Y, Fujita K, Kamataki T. Inhibition of benzo[*a*]pyrene-induced mutagenesis by (−)-epigallocatechin gallate in the lung of rpsL-transgenic mice. *Carcinogenesis* 1999; **20**: 421–4.
14. Kuroda Y, Hara Y. Antimutagenic and anticarcinogenic activity of tea polyphenols. *Mutat Res* 1999; **436**: 69–97.
15. Yang GY, Liao J, Kim K, Yurkow EJ, Yang CS. Inhibition of growth and induction of apoptosis in human cancer cell lines by tea polyphenols. *Carcinogenesis* 1998; **19**: 611–6.
16. Okabe S, Ochiai Y, Aida M, Park K, Kim S-J, Nomura T, Suganuma M, Fujiki H. Mechanistic aspects of green tea as a cancer preventive: effect of components on human stomach cancer cell lines. *Jpn J Cancer Res* 1999; **90**: 733-9.
17. Setiawan VW, Zhang ZF, Yu GP, Lu QY, Li YL, Lu ML, Wang MR, Guo CH, Yu SZ, Kurtz RC, Hsieh CC. Protective effect of green tea on the risks of chronic gastritis and stomach cancer. *Int J Cancer* 2001; **92**: 600–4.
18. Rao DN, Ganesh B, Dinshaw KA, Mohandas KM. A case-control study of stomach cancer in Mumbai, India. *Int J Cancer* 2002; **99**: 727–31.
19. Kono S, Ikeda M, Tokudome S, Kuratsune M. A case-control study of gastric cancer and diet in northern Kyushu, Japan. *Jpn J Cancer Res* 1988; **79**: 1067–74.
20. Ohno Y, Wakai K, Genka K, Ohmine K, Kawamura T, Tamakoshi A, Aoki R, Senda M, Hayashi Y, Nagao K, Fukuma S, Aoki K. Tea consumption and lung cancer risk: a case-control study in Okinawa, Japan. *Jpn J Cancer Res* 1995; **86**: 1027–34.
21. Imai K, Suga K, Nakachi K. Cancer-preventive effects of drinking green tea among a Japanese population. *Prev Med* 1997; **26**: 769–75.
22. Li H-C, Yashiki S, Sonoda J, Lou H, Ghosh SK, Byrnes JJ, Lema C, Fujiyoshi T, Karasuyama M, Sonoda S. Green tea polyphenols induce apoptosis *in vitro* in peripheral blood T lymphocytes of adult T-cell leukemia patients. *Jpn J Cancer Res* 2000; **91**: 34–40.
23. Miyoshi I, Kubonishi I, Yoshimoto S, Shiraishi Y. A T-cell line derived from normal human cord leukocytes by co-culturing with human leukemic T-cells. *Gann* 1981; **72**: 978–81.
24. Ehrlich G, Greenberg S, Abbot M. Detection of human T-cell lymphoma/

leukemia viruses. In: Innis M, Gelfand D, Sninsky J, White T, editors. PCR protocols. San Diego: Academic Press; 1990. p. 325–32.
25. Pisters KM, Newman RA, Coldman B, Shin DM, Khuri FR, Hong WK, Glisson BS, Lee JS. Phase I trial of oral green tea extract in adult patients with solid tumors. *J Clin Oncol* 2001; **19**: 1830–8.
26. Nagai M, Usuku K, Matsumoto W, Kodama D, Takenouchi N, Moritoyo T, Hashiguchi S, Ichinose M, Bangham CRM, Izumo S, Osame M. Analysis of HTLV-1 proviral load in 202 HAM/TSP patients and 243 asymptomatic HTLV-1 carriers: high proviral load strongly predisposes to HAM/TSP. *J Neurovirol* 1998; **4**: 586–93.
27. Yang CS, Chen L, Lee MJ, Balentine D, Kuo MC, Schantz SP. Blood and urine levels of tea catechins after ingestion of different amounts of green tea by human volunteers. *Cancer Epidemiol Biomarkers Prev* 1998; **7**: 351–4.
28. Mueller N, Okayama A, Stuver S, Tachibana N. Findings from the Miyazaki Cohort Study. *J Acquir Immune Defic Syndr Hum Retrovirol* 1996; **13**: S2–7.
29. Hisada M, Okayama A, Tachibana N, Stuver SO, Spiegelman DL, Tsubouchi H, Mueller NE. Predictors of level of circulating abnormal lymphocytes among human T-lymphotropic virus type I carriers in Japan. *Int J Cancer* 1998; **77**: 188–92.
30. Lee MJ, Wang ZY, Li H, Chen L, Sun Y, Gobbo S, Balentine DA, Yang CS. Analysis of plasma and urinary tea polyphenols in human subjects. *Cancer Epidemiol Biomarkers Prev* 1995; **4**: 393–9.
31. Ahmad N, Gupta S, Mukhtar H. Green tea polyphenol epigallocatechin-3-gallate differentially modulates nuclear factor kappaB in cancer cells versus normal cells. *Arch Biochem Biophys* 2000; **376**: 338–46.
32. Suzuki T, Hirai H, Murakami T, Yoshida M. Tax protein of HTLV-1 destabilizes the complexes of NF-kappa B and I kappa B-alpha and induces nuclear translocation of NF-kappa B for transcriptional activation. *Oncogene* 1995; **10**: 1199–207.
33. Yamaguchi K, Kiyokawa T, Nakada K, Yul LS, Asou N, Ishii T, Sanada I, Seiki M, Yoshida M, Matutes E. Polyclonal integration of HTLV-I proviral DNA in lymphocytes from HTLV-I sero-positive individuals: an intermediate state between the healthy carrier state and smoldering ATL. *Br J Haematol* 1988; **68**: 169–74.

Radical Species in DNA Strand-Cleavage Caused by Dihydropyrazines

Nobuhiro KASHIGE,[a] Toru TAKEUCHI,[b] Shigenobu MATSUMOTO,[c] Shinji TAKECHI,[d] Fumio MIAKE,[a] and Tadatoshi YAMAGUCHI*,[d]

[a] *Faculty of Pharmaceutical Sciences, Fukuoka University; Fukuoka 814–0180, Japan:* [b] *Department of Environmental Medicine, Kagoshima University Graduate School of Medical and Dental Sciences; Kagoshima 890–8544, Japan:* [c] *Redox Regulation Research Group, Tokyo Metropolitan Institute of Gerontology; Itabashi-ku, Tokyo 173–0015, Japan: and* [d] *Department of Hygiene, Miyazaki Medical College; Kiyotake-cho, Miyazaki 889–1692, Japan.*

Received October 14, 2004; accepted December 28, 2004; published online December 28, 2004

Dihydropyrazines (DHPs), which generate hydroxyl and carbon-centered radicals, cleaved DNA single-strand. It is new knowledge that DHPs were recently determined to produce 8-hydroxydeoxyguanosine. The remarkable increase in the DNA strand-cleavage activity upon the addition of Cu^{2+} suggests that the primary reactive species is carbon-centered radicals rather than the hydroxyl radical generated the initiation reaction. This proposal was in fair agreement with of the observed carbon-centered radical signal intensity, but an effect was not observed with the increase in the hydroxyl radical signal intensity.

Key words dihydropyrazine; DNA strand-cleavage; carbon-centered radical; hydroxyl radical

Dihydropyrazines (DHPs) revealed the single strand-cleavage[1] of covalently closed circular DNA of plasmid pBR322, especially in the presence of Cu^{2+}. This cleavage was determined to be initiated by the radical species generated from DHPs. Therefore, further investigation of the reactivity of DHPs continues our laboratory.

DNA damage is closely related to the variety of biological phenomena such as mutagenesis, carcinogenesis, aging and radiation effects. A better understanding of the mechanism of the biological effects caused by DHPs is of great interest, because DHPs were derived from sugar and universally existed in human body, and consequently might caused various internal injuries *in vivo*.[2] The chemical reactivity[3,4] and the biological effects[2,5] of DHPs have been elucidated. The electron spin resonance (ESR) spectrum of DHPs showed the cogeneration of four radical species[6] such as ·OH, ·OOH, ·CHR_2 and ·CR_3 at the same time. Furthermore, the specificity[7] of the nucleotide sequence DNA strand cleavage sites produced by DHPs has been identified. However, whether oxygen radica'ls or carbon-centered radicals (C-radicals) primarily involved in the DNA strand-cleavage remains unclear. There are a number of reports of DNA strand-cleavage due to reactive oxygen species, including hydroxyl radical, however, there have been few reports related to C-radical.[8—11] The DNA damage caused by the copper-peroxide complex provides a unique example.[12]

Herein, we use the results of DNA strand-cleavage activity and the ESR spectra with a spin-trapping agent to propose that the radical species that attacked the DNA strand formed 8-hydroxydeoxyguanosine (8-OHdG).

MATERIALS AND METHODS

Synthesis of Dihydropyrazine Derivatives The dihydropyrazine derivatives (Fig. 1) employed were all synthesized by condensation of diketones and diamines. 2,3-Dihydro-5,6-dimethylpyrazine (DHP-1), 2,3-dihydro-2,5,6-trimethylpyrazine (DHP-2) and 3-hydro-2,2,5,6-tetramethylpyrazine (DHP-3) were synthesized by the method of Yamaguchi *et al.*[1] 2,3,-Dihydro-5-methy, 6-phenylpyrazine[13] (DHP-4) was also synthesized by similar method.

Assay of DNA Strand-Breaking Activity The method of assaying the DNA strand-cleavage activity of DHPs, using a covalently closed circular duplex DNA of plasmid pBR32 (ccc-DNA) was previously described. [14]

ESR Spectroscopy of Dihydropyrazines The ESR spectra were recorded on a JES-FA200 spectrometer (JEOL Co., Tokyo) using a Mn^{2+} marker as an external standard, and an ES-LC12 flat cell (JEOL Co., Tokyo). The spectra were measured in a 50 mM Tris–HCl buffer (pH 7.1) using 5,5-dimethy-1-pyrroline *N*-oxide (DMPO) as a spin trapping agent, according to previous paper.[6] The relative values were summarized in Table 3. The instrumental condition were: field center 335.9 mT, scan width ±5 mT, modulation frequency 100 kHz, modulation width 0.14 mT, time constant 0.3 s, amplitude 7×100, microwave power 10 mW, and microwave frequency 9.427 GHz. The spectra were recorded at 30 min after mixing.

The Measurement of 8-Hydroxydeoxyguanosine The DNA samples for the measurement of 8-hydroxydeoxyguanosine (8-OHdG) were prepared as follow. The reaction mixture (500 μl) containing 10 μg of pBR322 ccc-DNA and 20 mM DHP in 50 mM Tris–HCl buffer (pH 7.2) was incubated for 1 h with or without 1 mM $CuCl_2$. The reaction was stopped by the addition of 1ml cold ethanol, and the DNA product was precipitated at −80 °C for 1 h. The precipitated DNA was then dissolved in 0.3 M sodium acetate, and again precipitated with ethanol, rinsed in cold ethanol for 2 times, and dried. The amount of 8-OHdG was determined according to Takeuchi *et al.*[15] Briefly, DNA was heat-denatured and then digested sequentially with nuclease P1 and alkaline phosphatase. Quantities of 8-OHdG and deoxyguanosine (dG) were determined by high performance liquid chromatography with electrochemical detection and UV absorp-

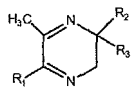

DHP-1 : $R_1 = CH_3$, $R_2 = R_3 = H$
DHP-2 : $R_1 = R_2 = CH_3$, $R_3 = H$
DHP-3 : $R_1 = R_2 = R_3 = CH_3$
DHP-4 : R_1 = Ph, $R_2 = R_3 = H$

Fig. 1. Chemical Structures of Dihydropyrazines Used

* To whom correspondence should be addressed. e-mail: yamaguti@med.miyazaki-u.ac.jp

tion. 8-OHdG levels were expressed as the molar ratio of 8-OHdG per 10^5 dG.

RESULTS

Oxygen radicals are well known to attack and damage single-stranded DNA. However, there have been very few previous reports on the activity of C-radicals. This may be because there is no standard substance for the resultant products from the reaction of nucleic base with C-radicals. Herein, we attempted to explain C-radical participation in DNA damage.

Thus far the degradation of DNA by ·OH regard with Cu^{2+} has been reported to be the reactive species. This has been observed for the copper(II)–phenanthroline complex[16] in the presence of reducing agents such as NADH, thiol, ascorbate, and the ternary complex (copper–phenanthroline–DNA)[17] in the presence of DNA, furthermore, the hydroperoxide–dicopper(II) complex[12,18] produced from the reaction of Cu(I) with H_2O_2. The characteristics of DHPs were noteworthy because DNA damages induced by copper and the reactive oxygen species have a significant correlation with the DNA degradation by DHPs. DHP has three functions; reducing ability, chelating ability in the presence of copper, and the ability to independently generate ·OH and C-radicals. Therefore, certain mechanisms of the DNA damage by DHPs must be considered.

The single-strand cleavage activities of DHPs in the presence or absence of Cu^{2+} are summarized in Table 1. The relative amounts of remaining ccc-DNA after 1 or 3 h of incubation time are shown as an index of activity. The order of DNA strand-cleavage activity was DHP-3>DHP-2>DHP-4>DHP-1 in the presence of Cu^{2+}, although the difference in the cleavage activity for DHP-1—4 was hard to recognized in the absence of Cu^{2+}.

It is already apparent[1] that Cu^{2+} converted into Cu^{1+} by the reducing ability of DHPs. The relationship between the reducing ability shown in Fig. 2 and the cleavage activity of DHPs was examined. The reducing ability for DHPs decreases in the order: DHP-3>DHP-2>DHP-1>DHP-4. The result indicated that the cleaving activity can consider to be similar to the strength of electronic release ability, because DHPs converted into C-radical by electron releasing.

Experiment results show for the first time that 8-OHdG was produced by DHPs. In the comparison (Table 2) of the amounts of 8-OHdG formed by DHPs, although the formed amounts have too big difference on the absence or presence of Cu^{2+}, the order of the formation of 8-OHdG is DHP-4>DHP-3>DHP-2=DHP-1 either with or without Cu^{2+}. DHP-4 formed the greatest amounts of 8-OHdG. The amounts of 8-OHdG formed increased remarkably upon addition of Cu^{2+}. Addition of Cu^{2+} increased the amount of 8-OHdG formed by about 40 times in the both cases of DHP-1 and DHP-2. In addition, the amount of 8-OHdG formed was increased by about 90 times and about 100 times in the cases of DHP-3 and of DHP-4, respectively. However, this increase can not be equated with the amount of 8-OHdG

Table 1. DNA Single-Strand Cleavage by Dihydropyrazines in Absence or Presence of Cu^{2+}

Compound	Conc. (mM)	ccc-DNA remaining (%)	
		With Cu^{2+} for 1 h	Without Cu^{2+} for 3 h
Control	—	100	100
DHP-1	0.1	95	100
	1	47	82
	5	—	—
	10	21	60
	20	0	82[a]
DHP-2	0.1	92	100
	1	44	91
	5	—	—
	10	0	63
	20	0	77[a]
DHP-3	0.1	64	97
	1	0	91
	5	—	—
	10	0	71
	20	0	80[a]
DHP-4	0.1	93	99
	1	71	96
	5	17	86
	10	0	79
	20	0	91[a]

Plasmid pBR322 ccc-DNA was incubated with various concentrations of DHP in 50 mM Tris–HCl buffer (pH 7.2) at 37 °C for 1 h with 1 mM $CuCl_2$ or for 3 h without $CuCl_2$. The examination of each at 20 mM of DHPs was used in order to obtain a sample for the measurement of 8-OHdG amount. *a*) Data taken at 1 h. It is indicated that ccc-DNA was converted into linear DNA *via* open-circular DNA, then the breakage activity is as strong as the amount of remaining ccc-DNA is small.

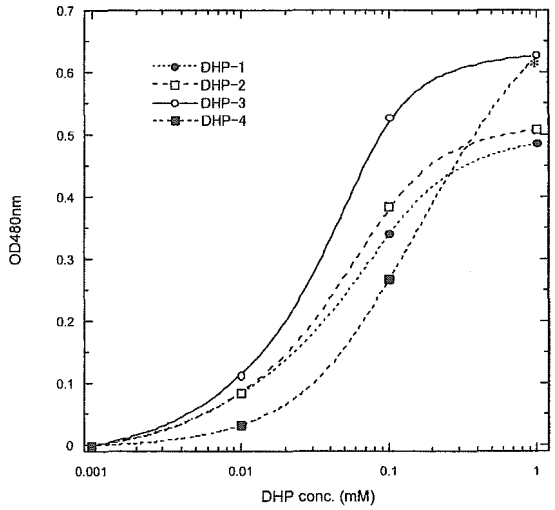

Fig. 2. Comparison of the Reduction Ability of Dihydropyrazines Which Convert Cu^{2+} into Cu^{1+}

Various concentrations of DHPs were incubated with 100 μM bathocuproine disulfonate at 37 °C in 50 mM Tris–HCl buffer (pH 7.2) for 1 h in the presence of 1 mM $CuCl_2$. The OD at 480 nm is showing the quantity of resulted Cu(I)–bathocuproine complex. *At 1 mM of DHP-4, precipitation was caused in reaction solution, and accurate measurement was imposible.

Table 2. The Amount 8-Hydroxydeoxyguanosine Formed by Dihydropyrazines

	Without Cu^{2+}	With Cu^{2+}
Control	2.14	50.11
DHP-1	21.73	761.04
DHP-2	21.41	774.23
DHP-3	22.80	1874.46
DHP-4	25.26	2510.82

8-OHdG levels were expressed as the molar ratio of 8-OHdG per 10^5 dG.

formed or with the cleavage activity in the DHPs, because the relation between the order (DHP-3>DHP-2>DHP-4>DHP-1) of the DNA cleavage activity and the order (DHP-4>DHP-3≫DHP-2=DHP-1) of the amount of 8-OHdG formed showed the clear deference in the presence of Cu^{2+}. Thus, the amount of ·OH, which produced 8-OHdG, was not in good agreement with the order of the DNA breakage activity. This indicated that the participation of C-radical was strongly suggested in DNA cleavage reaction by DHPs. Because no superoxide anion radical was detected in ESR, although 8-OHdG also was produced by active oxygens ($\cdot O_2^-$ or singlet state oxygen) except for ·OH.

The ESR spectrum of DHP-1 showed in Fig. 3 as an example. The two radical signals were detected as adducts of DMPO used as a spin trapping agent. The relative intensity of hydroxyl radical (·OH) and C-radicals generated from DHPs was showed in Table 3. The strength of C-radical intensity for ·OH increased remarkably upon addition of Cu^{2+}, especially, in the DHP-3 and -4 (increased in about *ca.* 9 and *ca.* 25 times, respectively) as shown in Table 3. This occurred despite the ·OH signal showed no rise. The increment of C-radical in DHP-4 was most remarkably in the presence of Cu^{2+}. This result corresponds well to the DNA cleavage activity that was elevated in the presence of Cu^{2+} as shown in Table 1. The order of relative intensity of the C-radical was in good agreement with that of the amount of 8-OHdG formed. However, it was not in good agreement with that of DNA cleavage activity.

DISCUSSION

The presumed mutual interaction of DHP and Cu^{2+} was shown in Chart 1. The DHP reached an unstable state by releasing an electron, subsequently generating radicals, and finally resolved. At the same time, the dissolved O_2 captured a released electron, and converted into ·OH *via* $\cdot O_2^-$ concomitantly with the formation of Cu^{1+} from the reduction of Cu^{2+}.

In the ESR spectra of DHPs, using DMPO as a spin trapping agent, $\cdot O_2^-$ was not detected, and further, the inhibition effect of SOD was not observed. Thus, a directly attack of $\cdot O_2^-$ to the DNA was excepted. In the presence of Cu^{2+}, the DNA strand cleavage activity (Table 1), the formed amounts of 8-OHdG (Table 2) and the ESR signal intensity of radicals increased remarkably. The ESR signal intensity was variable related to the concentration of Cu^{2+}. The intensity increased by about 20% at the 0.08 of molar-ratio of Cu^{2+} to DHP, however it decreased by about 80% at the 0.8 molar ratio. At the 0.01 of the molar ratio, no effect was observed. As the concentration of Cu^{2+} increased, the precipitate of the DHP compound chelated to Cu^{2+} was produced and radical generation terminated. Thus, the presence of an adequate amount Cu^{2+} was thought to be necessary in order to cause radical generation. In the DNA cleavage reaction, binding of Cu^{2+} to pBR322 ccc-DNA was confirmed,[18] producing the Cu^{2+}-DNA complex, which was broken more easily than free DNA. Therefore, the effect of Cu^{2+} in existence of DNA strand, differ from that shown in the ESR measurement without the DNA strand. As shown in Chart 1, the reproduced Cu^{2+} was utilized in the reaction system, indicating that

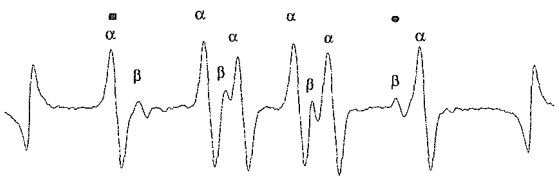

Fig. 3. The ESR Spectrum of DMPO-Adduct of 2,3-Dihydro-5,6-dimethylpyrazine (DHP-1) in the Presence of Cu^{2+}

ESR spectrum obtained from the reaction of DHP-1 (6 mM) with $CuCl_2$ (0.01 mM) in the presence of DMPO (100 mM) at pH 7.1 (50 mM Tris–HCl buffer) (DHP-1+Cu^{2+}, Table 3). Spectrum was assigned to DMPO adducts of hydroxyl (β) and carbon-centered (α) radicals. Peaks indicated with (●; hydroxyl radical) and (■; carbon-centered radical) were used for the determination of the relative intensities of DMPO adducts.

Table 3. The Relative Intensity of Hydroxyl and Carbon-Centered Radicals Generated from Dihydropyrazine

Compound	Hydroxyl radical	Carbon-centered radical
DHP-1	0.21 (27%)	0.56 (73%)
DHP-1+Cu^{2+}	0.51 (13%)	3.49 (87%)
DHP-2	0.35 (31%)	0.78 (69%)
DHP-2+Cu^{2+}	0.58 (21%)	2.12 (79%)
DHP-3	1.63 (16%)	8.73 (84%)
DHP-3+Cu^{2+}	1.45 (10%)	12.70 (90%)
DHP-4	1.39 (27%)	3.75 (73%)
DHP-4+Cu^{2+}	1.05 (4%)	25.76 (96%)

The values represent the peak heights of the first signal of carbon-centered radical-DMPO adducts and the fourth signal of hydroxyl radical-DMPO adducts (see Fig. 3). The spectra were measured under conditions described in Materials and Methods. Signal intensities were calibrated by comparison with a standard Mn^{2+} marker. To confirm the relative intensities of these radical aducts, computer simulation of spectra were performed using these values.

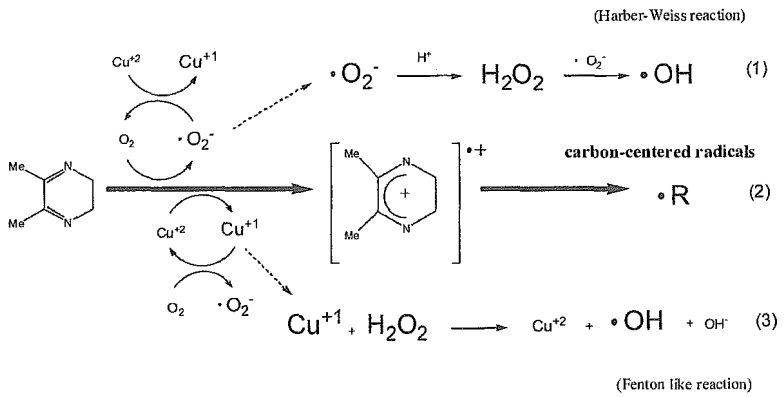

Chart 1. The Mutual Interaction of Dihydropyrazines and Cu^{2+}

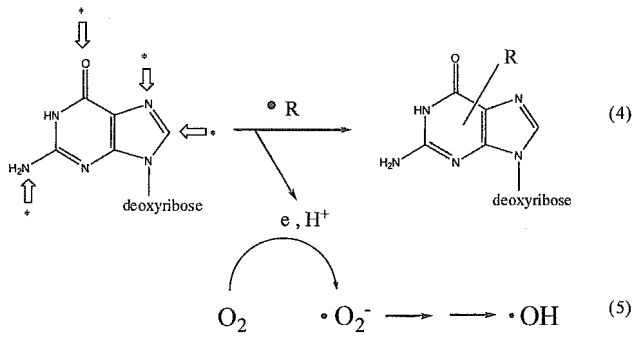

*Arrow marks show the parts which may be alkylated.

Chart 2. Alkylation of Nucleic Base Such as Guanylic Acid Part in DNA by Carbon-Centered Radical and Then the Generation of Hydroxyl Radical

small amounts of Cu^{2+} are sufficient to generate the radicals. It was presumed that Eqs. 1 and 2 in Chart 1 were occurred in the absence of Cu^{2+}, and in the presence, Eq. 2 was amplified and Eq. 3 was newly added. The DNA cleavage reaction was examined to determine whether ·OH or C-radical primarily involved in DNA breakage reaction. The order (DHP-3>DHP-2>DHP-4>DHP-1) of the cleavage activity is a considerable difference from the order (DHP-4>DHP-3 ≫DHP-2=DHP-1) of the formed 8-OHdG.

It is differ from the order of cleavage activity that the amount of formation of 8-OHdG is almost equivalent at DHP-1 and DHP-2 as shown in Table 2. In the case of DHP-4, the C-radical signal increased upon addition of Cu^{2+} and the ratio of ·OH reached very low level, as shown in Table 3. The amount of 8-OHdG formed was, however, the greatest. Chart 2 depicts an alternative pathway to explain the seeming inconsistency. The amount 8-OHdG formed may be explained by Eqs. 4 and 5 in Chart 2. Table 3 shows the relative signal intensities of C-radical were 73—96%, whereas that of the ·OH was low. Thus, participation of C-radical cannot be accounted for, and the effect at the time of copper addition cannot be explained. The ESR spectra on DHP-3 and DHP-4 with or without of Cu^{2+}, show a comparison of signals in which an increase in ·OH is not observed and further that C-radical increases greatly, as shown in Table 3. In our previous paper,[7] we reported that the most preferentially cleaved sites induced by DHPs were at purine/pyrimidine-guanine (5′->3′) sequences after being heated with aqueous piperidine. Therefore, the hypothesis as shown in Chart 2 was estimated. The C-radical produced from DHPs attacked to DNA strand, especially in the deoxyguanilate regions, which may be possible binding sites for Cu^{2+}. Further, the Cu^{2+}–DNA complex may oxidize DHPs in vicinities to generate ·OH and C-radical, which is finally responsible for the DNA damage. The electron emitted as shown in Eq. 4 makes ·OH *via* $\cdot O_2^-$ (Eq. 5).

The formation of O^6-alkylguanie[20] and, 8-OHdG[21] and 2-hydroxydeoxyadenosine[21] are known to cause a transition of GC to AT and a transversion of GC to TA. The data related to mutagenesis in *Escherichia coli* has been previously obtained (the data not shown; the base pair substitutions GC to AT and GC to TA appeared to be predominant.). Thus, the alkylation shown in Eq. 4 is thought to be performed by the C-radical.

The DNA cleavage reaction by DHPs in the presence of Cu^{2+} is thought to be induced primarily by the C-radical, as shown in Charts 1 and 2. Furthermore, it was determined that there is no accompanying auxiliary action of ·OH.

Definitive evidence which ·OH participate only a few in the DNA cleaving activity has been obtained. ESR spectrum observed in a degassed solution showed the diminished intensity of ·OH signal. In spite of an anaerobic conditions, the assay of the cleaving activity was recognized as similar as a control in the air. The detailed study should be published in a following paper.

Free radical species such as ·OH and C-radical from DHPs attacked to DNA strand, and the resultant 8-OHdG and alkylated nucleic acid base adducts elicited various DNA damages (the degradation of DNA and mutagenesis, carcinogenesis, teratogen as genotoxic property). The present report focuses solely on DNA strand-cleavage activity. However, since it is known that C-radical react very rapidly with molecular oxygen, and the products formed from this reaction (such as peroxyl radicals) are generally considered to be more deleterious to biomolecules than the parent alkyl radical, certain unknown functions of DHPs were further expected. Data on the role of DHP has been obtained. That data contained certain cases that the effects by DHPs did not be inhibited by radical scavengers. Thus, the effect of DHPs is thought to be due to the chemical reactivities of DHPs, without the participation of radical species.

Further investigation on the biological activity of DHPs is currently underway.

Acknowledgements This work was supported in part by a Grant-Aid for Scientific Research (C) from the Japan Society for the Promotion of Science (JSPS).

REFERENCES AND NOTES

1) Yamaguchi T., Kashige N., Mishiro N., Miake F., Watanabe K., *Biol. Pharm. Bull.*, **19**, 1261—1265 (1996).
2) Yamaguchi T., Nomura H., Matsunaga K., Ito S., Takata J., Karube Y., *Biol. Pharm. Bull.*, **26**, 1523—1527 (2003).
3) Yamaguchi T., Eto M., Harano K., Kashige N., Watanabe K., Ito S., *Tetrahedron* **55**, 675—686 (1999).
4) Yamaguchi T., Ito S., Iwase Y., Watanabe K., Harano K., *Hetrocycles*, **51**, 2305—2309 (1999).
5) Takechi S., Yamaguchi T., Nomura H., Minematsu T., Nakayama T., *Mutat. Res.*, **560**, 49—55 (2004).
6) Yamaguchi T,. Matsumoto S., Watanabe K., *Tetrahedron Lett.*, **39**, 8311—8312 (1998).
7) Kashige N., Yamaguchi T., Miake F., Watanabe K., *Biol. Pharm. Bull.*, **23**, 1281—1286 (2000).
8) August O., Falijoni-Alario A., Leite L. C. C., Noberga F., *Carcinogenesis*, **5**, 781—784 (1984).
9) Leite L. C. C., August O., *Arch. Biochem. Biophys.*, **270**, 560—572 (1989).
10) August O., *Free Radic. Biol. Med.*, **15**, 329—336 (1993).
11) Hiramoto K., Inoue M., Maeda K., Kato T., Kikugawa K., *Jpn. J. Toxicol. Environ. Health*, **40**, 412—421 (1994).
12) Yamamoto K., Kawanishi S., *J. Biol. Chem.*, **264**, 15435—15440 (1989).
13) mp 36.0—37.5 °C (recrystalized from *n*-hexane), 92.4% yield. FAB-MS *m/z*: 172.1084 [$(M+H)^+$, $C_{11}H_{13}N_2$ (MW: 172.1079)].
14) Kashige N., Yamaguchi T., Mishiro N., Hanazono H., Miake F., Watanabe K., *Biol. Pharm. Bull.*, **18**, 653—658 (1995).
15) Takeuchi T., Nakajima M., Ohta Y., Mure K., Takeshita T., Morimoto K., *Carcinogenesis*, **15**, 1519—1523 (1994).
16) Gutteridge J. M. C., Hakkiwell B., *Biochemistry Pharmacology*, **31**,

2801—2805 (1982).
17) Goldstein S., Czapski G., *J. Am. Chem. Soc.*, **108**, 2244—2250 (1986).
18) Karlin K. D., Ghosh P., Cruse R. W., Faroop A., Gultneh Y., Jacobson R. R., Blackburn N. J., Strange R. W., Zubieta J., *J. Am. Chem. Soc.*, **110**, 6769—6780 (1988).
19) Kashige N., Kojima M., Nakajima Y., Watanabe K., Tachifuji A., *Agric. Biol. Chem.*, **53**, 677—684 (1990).
20) Horsfall M. J., Gordon A. J. E., Burns P. A., Zielenska M., van der Vliet G. M. E., Glickman B. W., *Environ. Mol. Mutagen*, **15**, 107—122 (1990).
21) Kamiya H., *Biol. Pharm. Bull.*, **27**, 475—479 (2004).

Free Radical Research, September 2005; 39(9): 905–911

Taylor & Francis
Taylor & Francis Group

Habitual exercise induced resistance to oxidative stress

KOJI NAKATANI[1,2], MASAHARU KOMATSU[2], TOYOHIRO KATO[2], TAKAO YAMANAKA[1], HIROAKI TAKEKURA[1], AKIRA WAGATSUMA[1], KOHJI AOYAMA[2], BAOHUI XU[2], TAKESHI HIRANO[3], HIROSHI KASAI[4], SEIICHI ANDO[5], & TORU TAKEUCHI[2]

[1]*Department of Physiological Sciences, National Institute of Fitness and Sports, Kanoya, Kagoshima 891-2393, Japan,* [2]*Department of Environmental Medicine, Graduate School of Medical and Dental Sciences, Kagoshima University, Sakuragaoka, Kagoshima 890-8544, Japan,* [3]*Graduate School of Engineering, The University of Kitakyushu, Kitakyushu, Fukuoka 808-0135, Japan,* [4]*Department of Environmental Oncology, School of Medicine, University of Occupational and Environmental Health, Kitakyushu, Fukuoka 807-8555, Japan, and* [5]*Department of Fisheries Science, Kagoshima University, Shimoarata, Kagoshima 890-0056, Japan*

Accepted by Professor N. Taniguchi

(Received 12 May 2005)

Abstract

We investigated whether habitual exercise (HE) modulates levels of oxidative DNA damage and responsiveness to oxidative stress induced by renal carcinogen Fe-nitrilotriacetic acid (Fe-NTA). During a ten week protocol, two groups of rats either remained sedentary or underwent swimming for 15–60 min per day, 5 days per week, with or without a weight equivalent to 5% of their body weight. Then we injected Fe-NTA and sacrificed the rats 1 h after the injection. We determined the activity of superoxide dismutase (SOD) in diaphragm and kidney, evaluated levels of 8-hydroxydeoxyguanosine (8OHdG), catalase, and glutathione peroxidase, and assayed OGG1 protein levels in kidney. SOD activity in the diaphragm and kidney was increased in HE rats. By itself, HE had no effect on the level of 8OHdG, but it did significantly suppress induction of 8OHdG by Fe-NTA, and the amount of suppression correlated with intensity of exercise. These results suggest that HE induces resistance to oxidative stress and, at least at the initiation stage, inhibits carcinogenesis.

Keywords: *Exercise, Fe-nitrilotriacetic acid, 8-hydroxydeoxyguanosine, OGG1, superoxide dismutase, swimming*

Abbreviations: *dG, deoxyguanosine; Fe-NTA, Fe-nitrilotriacetic acid; GSHPx, glutathione peroxidase; HE, habitual exercise; 8OHdG, 8-hydroxydeoxyguanosine; hMTH, human MutT homolog; OGG1, 8-oxoguanine-DNA glycosylase 1; ROS, reactive oxygen species; SOD, superoxide dismutase*

Introduction

Exercise, especially habitual aerobic exercise is considered essential to promote and maintain health [1]. By increasing energy consumption and decreasing body weight, exercise reduces obesity, a well-known risk factor for cancer [2]. On the other hand, exercise also increases oxygen uptake [3], of which as much as 2% may possibly be converted to reactive oxygen species (ROS) [4,5]. ROS are thought to be strongly implicated in carcinogenesis [6,7]. Thus, exercise may be a double-edged sword when wielded in the fight against cancer. Numerous studies have investigated whether exercise increases oxidative damage, especially oxidative DNA damage [8–11]. While

Correspondence: T. Takeuchi, Department of Environmental Medicine, Graduate School of Medical and Dental Sciences, Kagoshima University, Sakuragaoka, Kagoshima 890-8544, Japan, Tel: 81 99 275 5288. Fax: 81 99 265 8434. E-mail: takeuchi@m.kufm.kagoshima-u.ac.jp

ISSN 1071-5762 print/ISSN 1029-2470 online © 2005 Taylor & Francis Group Ltd
DOI: 10.1080/10715760500183300

exhausting exercise is reported to increase DNA damage [9,10] moderate aerobic exercise is reported not to increase, and may even decrease, oxidative DNA damage [8,11]. Some findings have indicated that exercise increases the expression of superoxide dismutase (SOD), a scavenger of ROS [12,13], and human MutT homolog (hMTH), a damaged nucleotide sanitization enzyme [14]. These findings suggest that moderate aerobic exercise is unlikely to be harmful and is probably beneficial for the prevention of ROS-related cancer. However, no reports have yet investigated whether exercise lessens the effects of oxidative stress, one of the major causes of cancer [6,7].

We investigated whether habitual exercise (HE) changes the levels of oxidative DNA damage in the kidney and, at the same time, whether it modulates responsiveness against oxidative stress induced by Fe-nitrilotriacetic acid (Fe-NTA), a potent renal carcinogen [15,16].

Materials and methods

Animals and exercise protocols

All procedures in the animal experiments were performed in accordance with the guidelines of the Guiding Principles for the Care and Use of Animals in the Field of Physiological Sciences, published by the Physiological Society of Japan. This study was approval by the Animal Committee of the National Institute of Fitness and Sports. Thirty-five five-week-old male Wistar rats were obtained from CLEA Japan (Japan). The rats were kept under controlled conditions that included maintaining room temperature at 22 ± 1°C and a diurnal cycle of 12 h darkness and 12 h light. Food and water were provided *ad libitum*. After being allowed a week to adapt to their new surroundings, the rats were randomly allocated to two groups: habitual exercise (HE; $n = 19$), and sedentary (Control; $n = 16$). As shown in Table I, rats in the HE group were subjected to swimming. In blue–gray plastic garbage containers filled with water, maintained at 33°C to an average water depth of 60 cm, they swam in groups of two or three. The duration of swimming was initially 15 min, gradually increasing towards a full 60 min for all HE rats by week 7. Up to week 6, all HE rats were able to swim for the current target period of 45 min with a weight equivalent to 5% of body weight attached at the front of the chest. When the time was increased to 60 min, 9 out of 19 rats could not complete the session with the weight attached. Thereafter, 10 rats continued to swim with the weight (hard HE group) and 9 rats without the weight (soft HE group). Control group rats were not subjected to any swimming.

Fe-NTA treatment

Ten weeks into the protocol, 4 days after the final day of swimming, in each group, half of the rats intraperitoneally received Fe-NTA (15 mg Fe/ kg body weight) as described by Toyokuni et al. [15], and the remaining rats were similarly injected with an equivalent volume of saline. One hour after the injection, the rats were sacrificed, and their organs removed, frozen in liquid nitrogen, and stored at − 80°C until analysis.

Determination of 8-hydroxydeoxyguanosine (8OHdG)

Kidney was homogenized with 10 volumes of Dulbecco's phosphate buffered saline (w/v), then 550 μl samples of homogenate were transferred to tubes and centrifuged at 3800*g* for 2 min. The pellets were assayed for 8OHdG determination. DNA extraction and digestion were done under anaerobic conditions as described by Nakajima et al. [17]. 8OHdG and deoxyguanosine (dG) were separated with HPLC and evaluated by electrochemical detection and UV detection using previously described methods [18]. The presence of 8OHdG was quantified as the ratio of 8OHdG per 10^5 dG.

Table I. Exercise protocol.

Week	Duration of swimming	Attached weight 5% of body weight	Frequency times/week
1	none	none	None
2	15 min	none to +	5
3	15 to 30 min	+	5
4	30 min	+	5
5 to 6	45 min	+	5
7 to 11	60 min	+ or −	5

After being allowed a week to adapt to new surroundings, a group of five- week- old rats started a daily regimen of HE. The duration of swimming was gradually increased from 15 to 60 min. All of rats could swim for 45 min with a weight, but 9 out of 19 rats could not complete 60 min swimming with a weight. Consequently, from week 7 to 11 these 9 rats swam without a weight. Ten rats swam with a weight throughout the HE experiment.

Determination of SOD activity

Tissue homogenates were prepared as described by Oh-ishi et al. [19]. Briefly, diaphragm or kidney was homogenized with 9 volumes of a buffer containing 0.25 mol/l sucrose, 10 mmol/l Tris-HCl pH 7.4 and 0.1 mmol/l EDTA (w/v). After centrifugation at 770*g* for 15 min, SOD activity in the supernatants was measured using WST SOD assay kits (Dojindo, Japan). SOD activity in the samples was calculated by comparison with known activities of purified SOD (Wako pure chemical, Japan).

Determination of catalase and glutathione peroxidase (GSHPx) activities

Kidney was homogenized with 4 volumes of 100 mmol/l Tris-HCl pH 7.4 (w/v), then the homogenates were centrifuged at 510*g* for 10 min. Enzyme activity in the supernatants were measured as previously described [20].

Determination of 8-oxoguanine-DNA glycosylase 1 (OGG1)

The presence of OGG1 protein in kidney tissue was evaluated by immunoblotting. Tissue homogenates were prepared using the method described by Potts et al. [21]. To get intense and clear signals, the samples were not heated prior to electrophoresis. As previously described, homogenate samples containing 150 μg protein were subjected, under reducing conditions, to 12.5% sodium dodecyl sulfate—polyacrylamide gel electrophoresis and then transferred onto PVDF membranes (Immobilon-P, Millipore, Bedford, MA) at 370 mA for 35 min [22]. Prior to immunoblotting, the proteins on the PVDF membranes were stained with 1% Ponceau S in 5% acetic acid at room temperature for 10 min. After de-staining with Buffer A (0.35 mol/l NaCl, 10 mmol/l Tris-HCl pH 8.0, 0.05% Tween 20), the membranes were blocked, for 60 min at room temperature, with buffer A containing 3% bovine serum albumin and then incubated overnight at 4°C with a 500-fold dilution of polyclonal antibody against helix-hairpin-helix PDV motif (aa260–aa271) of mouse OGG1 [23] with Can Get Signal (Toyobo, Japan). The membranes were washed three times with buffer A and then incubated for 60 min with a 2000-fold dilution of horseradish-peroxidase-conjugated anti-rabbit IgG (Amersham Biosciences, Buckinghamshire, UK) with Can Get Signal. The membranes were washed for 1 min with buffer A, evenly coated using the ECL system (Amersham Biosciences, UK) and then immediately exposed to Hyperfilm™ ECL (Amersham Biosciences, UK). The protein levels of rat OGG1 were determined using Science Lab 2003 Multi Gauge software Ver 2.2 (FUJIFILM, Japan). OGG1 protein levels were standardized against a calibration sample prepared from a kidney from one of the control rats, and this sample was used in every electrophoresis. The OGG1 protein band intensity value of each sample was divided by that of the standard sample.

Protein determination

Protein concentrations in tissue homogenates were evaluated with Bio Rad protein assay solution, and the protein concentrations in samples were calculated in relation to known concentrations of bovine serum albumin.

Statistical analyses

The differences between samples were analyzed by one-way ANOVA followed by Fisher's least significant difference test or student *t*-test: *p* values of less than 0.05 were considered significant. Data were presented as mean ± standard error (SE).

Results

Effects of HE on body weight

As Figure 1 shows, HE significantly suppressed increase in body weight. A difference in body weight between HE and control groups was apparent even after the first week. Although the difference was not significant, animals in the hard HE group rats were lighter than those in the soft HE group. Comparing the weight of the hard and soft HE groups, *p* values were 0.10 at week 9, and 0.08 at weeks 10 and 11.

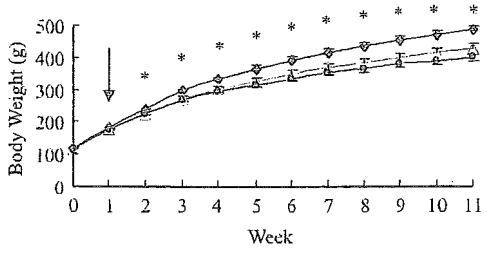

Figure 1. Changes in body weight during the experiment. Body weight was measured weekly and data is presented as means ± SE. Arrow indicates the point when HE was started. ◆, control group which did not swim throughout the experiment; Δ, soft HE group, which swam without a weight after week 7; ○, hard HE group, which swam with a weight throughout the eaperiment. Deashes indicate SE. *$p < 0.05$ when compared to control group.

8OHdG levels in kidney

As Figure 2 shows, HE did not increase 8OHdG levels in saline-injected rats. Although the difference was not significant ($p = 0.11$), the HE group showed lower 8OHdG levels than the control group. No significant difference was found in 8OHdG levels between hard and soft HE groups, i.e. 8OHdG levels in the hard group was $0.47 \pm 0.08/10^5$dG ($n = 5$) and in the soft group, $0.47 \pm 0.03/10^5$dG ($n = 4$).

8OHdG levels in kidney after Fe-NTA injection

As Figure 2 shows, Fe-NTA significantly increased 8OHdG in both HE and control groups. However, the resultant 8OHdG levels in the HE groups were significantly lower than in the control group. Furthermore, 8OHdG values correlated inversely with intensity of exercise (Figure 3, $r = 0.48$, $p < 0.05$). In the hard HE group the level of 8OHdG was significantly lower than in the control group, however the difference between the soft HE group and the control group did not reach significance.

Activities of antioxidant enzymes

As shown in Figure 4, without significance differences between the hard and soft groups, HE group diaphragm and kidney samples showed greater SOD activity. SOD activities in diaphragm of hard and soft HE groups were 10.7 ± 0.9 units/mg protein ($n = 5$) and 10.0 ± 0.7 units/mg protein ($n = 4$), and those in kidney were 20.5 ± 3.2 units/mg protein (n = 5) and 24.7 ± 1.1 units/mg protein (n = 4), respectively. There was no evidence that HE increased the activity

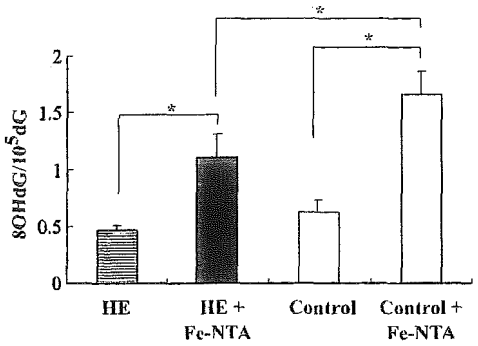

Figure 2. Effects of HE on 8OHdG levels in kidney. As described in Materials and methods, control ($n = 8$) and HE ($n = 9$) subgroups were injected with saline, and control +Fe-NTA ($n = 8$) and HE +Fe-NTA ($n = 10$) subgroups were injected with Fe-NTA. Rats were sacrificed 1 h after the final injection. 8OHdG was evaluated as described in Materials and methods. Dashes indicate SE. $^*p < 0.05$.

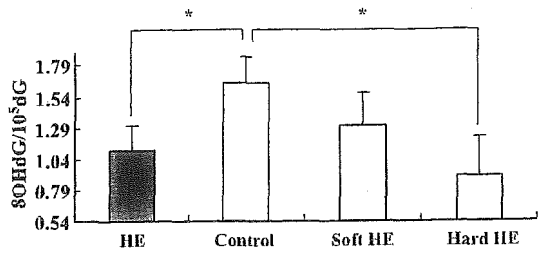

Figure 3. Effects of intensity of exercise on 8OHdG induction by Fe-NTA. The HE bar on the left indicates the mean for all rats injected with Fe-NTA after 10 weeks' swimming ($n = 10$). Control bar indicates the mean for 8 rats injected with Fe-NTA after 10 sedentary weeks. Soft HE and Hard HE bars indicate the means for 5 rats injected with Fe-NTA. Soft HE rats swam without a weight after week 7 and hard HE rats swam with a weight throughout the experiment. 8OHdG was evaluated as described in Materials and methods. The value $0.54/10^5$dG was the average 8OHdG level of rats injected with saline. Dashes indicate SE. $^*p < 0.05$.

of either catalase or GSHPx activities (Figure 5).

OGG1 protein levels in kidney.

Immunoblots of OGG1 protein in kidney samples revealed two major protein bands: one was calculated to be 46 kDa (# in Figure 6A); and the other to be 38 kDa (→ in Figure 6A). We assumed that OGG1 was indicated by the 38 kDa protein bands, which indicated that OGG1 protein levels were significantly lower in HE group samples (Figure 6A and C). As Figure 6B shows, the amounts of protein in the HE and control lanes were similar. No significant differences in OGG1 protein levels were observed between the hard (0.67 ± 0.06, $n = 5$) and soft (0.60 ± 0.06, $n = 4$) HE groups.

Discussion

Because HE is able to modulate the responsiveness to oxidative stress caused by higher ROS production in

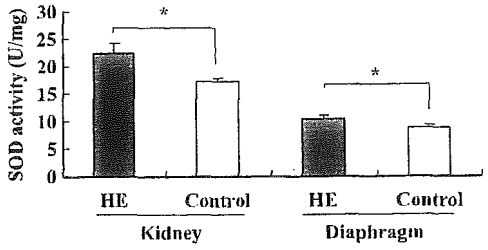

Figure 4. Effects of HE on SOD activities in kidney and diaphragm. As described in Materials and methods, SOD activity in kidney was evaluated in samples from sedentary (control, $n = 8$) and HE rats ($n = 9$) that had been injected with saline. SOD activity in diaphragm was determined for control ($n = 16$) and HE ($n = 19$) rats that had been injected with saline or Fe-NTA. Dashes indicate SE. $^*p < 0.05$.

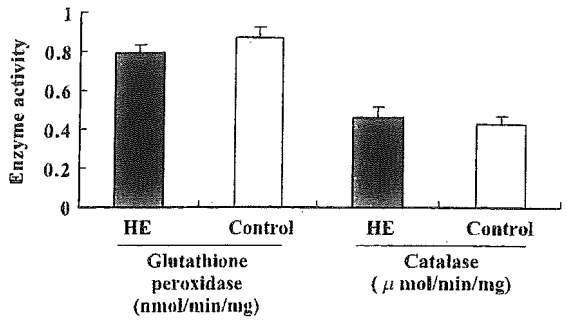

Figure 5. Effects of HE on catalase or glutathione peroxidase (GSHPx) activity in kidney. For Control ($n = 8$) and HE ($n = 9$) rats that had been injected with saline, the activity of catalase or GSHPx was evaluated as described in Materials and methods. Bars indicate SE.

the body, we investigated whether HE has any effect on ROS-related carcinogenesis. We originally wanted to test carcinogens that increase ROS production and induce cancer in lung tissue, where ROS production is most likely to increase during aerobic exercise. We could not, however, find any good candidate carcinogen for a lung-model experiment. We did discover Fe-NTA, a ROS-related carcinogen that reliably induces oxidative stress and cancer in kidney [15,16] and so designed an experiment to evaluate oxidative stress in kidney.

We measured 8OHdG levels in kidney and found that HE did not increase 8OHdG. We then

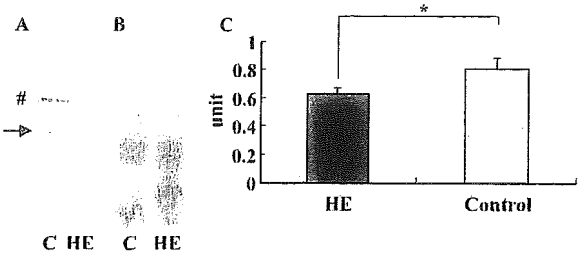

Figure 6. Effects of HE on OGG1 protein levels in kidney. (A) Immunoblots of OGG1. Samples (150 μg protein), from control or HE rats that had been injected with saline, were subjected to electrophoresis and then transferred on to membranes. OGG1 was detected with anti-OGG1 antibody and visualized as described in Materials and methods. Two major protein bands were detected: The molecular weight of the upper band (#) was 46 kDa, and the lower band (→) was 38 kDa. The right arrow (→) indicates OGG1. C lane, sample prepared from a control rat; HE lane, sample prepared from a hard HE rat. (B) Protein staining of the membrane. Proteins on the blotted membrane were stained with Ponceau S as described in Materials and methods. Lanes C and HE are the same lanes as those shown in Figure 6A. (C) OGG1 protein levels evaluated by immunoblotting. The unit indicates the ratio of OGG1 protein band intensity in samples against a standard sample, which was subjected to every electrophoresis. Dashes indicate SE. *$p < 0.05$.

investigated the effects of Fe-NTA and found that, similarly to previous reports [15,16], Fe-NTA increased 8OHdG in kidney. However, the 8OHdG level in the HE/Fe-NTA group was significantly lower than in the control/Fe-NTA group. When we analyzed the effects of intensity of exercise on 8OHdG induction, we found that lowest 8OHdG values in the hard HE group, significantly lower than in the control group. In the soft HE group, the 8OHdG level was between those in the hard HE and control groups, but not significantly lower than control values. This finding suggests that it was exercise, not just water immersion that had an effect on 8OHdG induction by Fe-NTA: amount of suppression correlated with intensity of exercise.

We then investigated why HE suppressed the 8OHdG induction by Fe-NTA. Because HE is reported to increase SOD activity in diaphragm [12,19], we evaluated SOD activities in diaphragm as well as in kidney; we found that HE increased SOD activities both in diaphragm and kidney. Increased SOD activity in the diaphragm indicates that the exercise loads were sufficient. It was not necessary to investigate precisely which SOD species were induced by HE because we were able to detect an overall increase in SOD activity in the HE group. We also tested catalase and GSHPx activity, but did not find any increase due to HE. The findings are in good agreement with that of Gunduz et al. in which they found that long-term daily swimming increased SOD activity but not catalase or GSHPx activity in kidney [24]. Other research suggests that, because the kidneys of Fe-NTA-injected rats become swollen and congestive/hyperemic, after injection of Fe-NTA, the activities of antioxidant enzymes in kidney are decreased [25,26]: consequently, we present data only from saline injected rats.

We also investigated whether HE increased 8OHdG repair activity. Because 8OHdG is mostly removed by OGG1 [27,28], we evaluated OGG1 protein levels in kidney samples. Fe-NTA injection is reported to modulate OGG1 activity in kidney [16], thus we investigated OGG1 protein levels in saline injected rats. OGG1 protein levels were lower in the HE group, a result that agrees well with our previous finding that HE decreases the expression of OGG1 [29]. We speculate that the mechanisms which bring about the lower levels of OGG1 that are associated with HE involve an increase in SOD, which may reduce ROS and decrease the generation of 8OHdG. This assumption is supported by the tendency for 8OHdG values in HE rats to be lower than those in control rats. These lower levels of 8OHdG in HE rats might have decreased the need for OGG1, because cells did not have to repair 8OHdG as efficiently as

control rats. This could plausibly account for the lower levels of OGG1 in HE rats. Our previous finding that HE decreased OGG1 levels [29] supports this speculation. In another previous finding, in contrast to OGG1, hMTH increased in an HE group [14]: as a result 8OHdG generation may have been decreased even more, resulting in a further decrease in OGG1.

In conclusion our findings suggest that HE suppresses induction of 8OHdG by Fe-NTA, mostly due to the efficient removal of superoxide by SOD, which suppresses Fe reduction. Associated with the intensity of HE in our protocol, we found no increase in oxidative DNA damage. Our results suggest that HE induces resistance to oxidative stress and suppresses the initiation step of carcinogenesis due to ROS. At the same time HE suppresses increases in body weight. These findings indicate that HE is beneficial for cancer prevention.

Acknowledgements

The authors express thanks to Dr Shinya Toyokuni (Department of Pathology and Biology of Diseases, Graduate School of Medicine, Kyoto University) for his helpful comments on the preparation of Fe-NTA. The authors also express thanks to Mr David Eunice for copyediting the manuscript. This work was supported by Grand-in-Aid for Scientific Research awarded by the Ministry of Education, Science, Sports and Culture of Japan (#14370140 and #16659149).

References

[1] Centers for Disease Control, National Center for Chronic Disease Prevention and Health Promotion Physical activity and good nutrition: Essential elements to prevent chronic diseases and obesity. Nutr Clin Care 2003;6:135–138.

[2] Stein CJ, Colditz GA. Modifiable risk factors for cancer. Br J Cancer 2004;90:299–303.

[3] Sen CK. Antioxidants in exercise nutrition. Sports Med 2001;31:891–908.

[4] Inoue M, Sato EF, Nishikawa M, Park AM, Kira Y, Imada I, Utsumi K. Mitochondrial generation of reactive oxygen species and its role in aerobic life. Curr Med Chem 2003;10:2495–2505.

[5] Wickens AP. Ageing and the free radical theory. Respir Physiol 2001;128:379–391.

[6] Halliwell B. Oxygen and nitrogen are pro-carcinogens. Damage to DNA by reactive oxygen, chlorine and nitrogen species: Measurement, mechanism and the effects of nutrition. Mutat Res 1999;443:37–52.

[7] Kasai H. Chemistry-based studies on oxidative DNA damage: Formation, repair, and mutagenesis. Free Radic Biol Med 2002;33:450–456.

[8] Inoue T, Mu Z, Sumikawa K, Adachi K, Okochi T. Effect of physical exercise on the content of 8-hydroxydeoxyguanosine in nuclear DNA prepared from human lymphocytes. Jpn J Cancer Res 1993;84:720–725.

[9] Poulsen HE, Weimann A, Loft S. Methods to detect DNA damage by free radicals: Relation to exercise. Proc Nutr Soc 1999;58:1007–1014.

[10] Tsai K, Hsu TG, Hsu KM, Cheng H, Liu TY, Hsu CF, Kong CW, Oxidative DNA damage in human peripheral leukocytes induced by massive aerobic exercise. Free Radic Biol Med 2001;31:1465–1472.

[11] Kasai H, Iwamoto-Tanaka N, Miyamoto T, Kawanami K, Kawanami S, Kido R, Ikeda M. Life style and urinary 8-hydroxydeoxyguanosine, a marker of oxidative DNA damage: Effects of exercise, working conditions, meat intake, body mass index, and smoking. Jpn J Cancer Res 2001;92:9–15.

[12] Powers SK, Criswell D, Lawler J, Martin D, Ji LL, Herb RA, Dudley G. Regional training-induced alterations in diaphragmatic oxidative and antioxidant enzymes. Respir Physiol 1994;95:227–237.

[13] Yamashita N, Hoshida S, Otsu K, Asahi M, Kuzuya T, Hori M. Exercise provides direct biphasic cardioprotection via manganese superoxide dismutase activation. J Exp Med 1999;189:1699–1706.

[14] Sato Y, Nanri H, Ohta M, Kasai H, Ikeda M. Increase of human *MTH1* and decrease of 8-hydroxydeoxyguanosine in leukocyte DNA by acute and chronic exercise in healthy male subjects. Biochem Biophys Res Commun 2003;305:333–338.

[15] Toyokuni S, Mori T, Hiai H, Dizdaroglu M. Treatment of Wistar rats with a renal carcinogen, ferric nitrilotriacetate, causes DNA-protein cross-linking between thymine and tyrosine in their renal chromatin. Int J Cancer 1995;62:309–313.

[16] Yamaguchi R, Hirano T, Asami S, Chung MH, Sugita A, Kasai H. Increased 8-hydroxyguanine levels in DNA and its repair activity in rat kidney after administration of a renal carcinogen, ferric nitrilotriacetate. Carcinogenesis 1996;17:2419–2422.

[17] Nakajima M, Takeuchi T, Morimoto K. Determination of 8-hydroxydeoxy-guanosine in human cells uncer oxygen-free conditions. Carcinogenesis 1996;17:787–791.

[18] Takeuchi T, Nakajima M, Ohta Y, Mure K, Takeshita T, Morimoto K. Evaluation of 8-hydroxydeoxyguanosine, a typical oxidative DNA damage, in human leukocytes. Carcinogenesis 1994;15:1519–1523.

[19] Oh-ishi S, Toshinai K, Kizaki T, Haga S, Fukuda K, Nagata N, Ohno H. Effects of aging and/or training on antioxidant enzyme system in diaphragm of mice. Respir Physiol 1996;105:195–202.

[20] Takeuchi T, Nakajima M, Morimoto K. Establishment of a human system that generates O_2^- and induces 8-hydroxydeoxyguanosine, typical of oxidative DNA damage, by a tumor promotor. Cancer Res 1994;54:5837–5840.

[21] Potts RJ, Watkin RD, Hart BA. Cadmium exposure down-regulates 8-oxoguanine DNA glycosylase expression in rat lung and alveolar epithelial cells. Toxicology 2003;184:189–202.

[22] Komatsu M, Sumizawa T, Mutoh M, Chen ZS, Terada K, Furukawa T, Yang XL, Gao H, Miura N, Sugiyama T, Akiyama S. Copper-transporting P-type adenosine triphosphatase (ATP7B) is associated with cisplatin resistance. Cancer Res 2000;60:1312–1316.

[23] Hirano T, Kudo H, Doi Y, Nishino T, Fujimoto S, Tsurudome Y, Ootsuyama Y, Kasai H. Detection of a smaller, 32-kDa 8-oxoguanine DNA glycosylase 1 in 3′-methyl-4-dimethylamino-azobenzene-treated mouse liver. Cancer Sci 2004;95:118–122.

[24] Gunduz F, Senturk UK, Kuru O, Aktekin B, Aktekin MR. The effect of one year's swimming exercise on oxidant stress and antioxidant capacity in aged rats. Physiol Res 2004;53:171–176.

[25] Iqbal M, Athar M. Attenuation of iron-nitrilotriacetate (Fe-NTA)-mediated renal oxidative stress, toxicity and hyperproliferative response by the prophylactic treatment of rats with garlic oil. Food Chem Toxicol 1998;36:485–495.

[26] Singh D, Chander V, Chopra K. Protective effect of naringin, a bioflavonoid on ferric nitrilotriacetate-induced oxidative renal damage in rat kidney. Toxicology 2004;201:1–8.

[27] Nishimura S. Involvement of mammalian OGG1(MMH) in excision of the 8-hydroxyguanine residue in DNA. Free Radic Biol Med 2002;32:813–821.

[28] Shinmura K, Yokota J. The OGG1 gene encodes a repair enzyme for oxidatively damaged DNA and is involved in human carcinogenesis. Antioxid Redox Signal 2001;3:597–609.

[29] Asami S, Hirano T, Yamaguchi R, Itoh H, Kasai H. Reduction of 8-hydroxyguanine in human leukocyte DNA by physical exercise. Free Radic Res 1998;29:581–584.

0163-4984/05/10700–0000 $30.00

Differentiation, Distribution, and Chemical State of Intracellular Trace Elements in LAD2 Mast Cell Line

KAZUKO NAKASHIMA,*[,1] TORU TAKEUCHI,[2] AND TARO SHIRAKAWA[1]

[1]Kyoto University School of Public Health, Yoshida-Konoe, Sakyo, Kyoto 606-8501, Japan; and [2]Department of Environmental Medicine, Kagoshima University Graduate School of Medical and Dental Sciences; 8-35-1, Sakuragaoka, Kagoshima 890-8544, Japan

Received December 16, 2004; Revised January 12, 2005; Accepted February 4, 2005

ABSTRACT

Oxidation state changes of metallic ions are involved in the generation and biological defense against reactive oxygen species. The relationship between allergy and oxidative damage by metallic elements was studied by X-ray fluorescence analysis using a mast cell line. The distribution of metallic elements is changed by the induction of reactive oxygen species. In mast cells, the degranulation leading to antigen or calcium ionophore stimulation is related to excessive accumulation of iron and to its chemical state. X-ray absorption near-edge structure spectroscopy showed that the oxidation state of iron in the cells shifted from Fe(II) to Fe(III) in degranulation. This finding might have implications for understanding the mechanisms involved in IgE-mediated cell responses as seen in allergic reaction.

Index Entries: Trace elements; degranulation; mast cell; synchrotron radiation; IgE.

INTRODUCTION

Various types of immune cell derive from undifferentiated stem cells. These differentiate into various cell lineages under the influence of

*Author to whom all correspondence and reprint requests should be addressed.

microenvironmental factors *(1)*. Some of these factors involve trace elements, which are at the active center of many enzymatic systems. A positive correlation between the severity of symptoms among asthmatic patients and the level of metallic particles in the air was found in an epidemiological study. Some metals, including transition metal ions and its compounds, have been found to cause adverse effects on human health. Also, it has been determined that several metal ions activated mast cells and enhanced allergen-mediated activation *(2)*.

Mast cells are important effectors in immunogloblin-E (IgE)-mediated allergic reactions and in inflammatory processes because of to their ability to secrete numerous cytokines *(3,4)*. Activated mast cells can produce several pro-inflammatory cytokines *(5–7)*. Many researchers have so far paid attention to the kinetics of intracellular calcium. It was thought that trace elements work in conjunction with other intracellular elements. Thus, we sought to determine the effect of metals and transition metal ions on the activation and enhancement of mast cells.

The present work is a pilot study of the intracellular distribution of trace elements in immune cells. We believe that our results will bring new light on allergy research.

EXPERIMENT

Reagents

The anti-hapten 4-hydroxy-3 iodo-5-nitrophenylacetic acid (NIP)–IgE, NIP–BSA (bovine serum albumin), and the calcium ionophore ionomycin were purchased from Sigma Chemical Co. (St Louis, MO). Stem-Pro-34 serum-free medium (SFM) complete medium, its nutrient supplement, and L-glutamine were purchased from Invitrogen Corp. (Gibco).

Materials

The human mast cell line LAD2 was selected for this study. This cell line has the same characteristics as human mast cells *(8)*. The cells were treated with some reagents to induce aggregation of the high-affinity IgE receptor (FcεRI) and to induce degranulation by release of chemical mediators, causing acute allergic inflammation. Cells were sensitized with 1 µg/mL human anti-NIP IgE for 30 min. Then, it was stimulated for 30 min by 1 ng/mL NIP-BSA to crosslink IgE and induce degranulation. Ionomycin was dissolved in dinethyl sulfoxide (DMSO) and added as a chemical stimulant to a final concentration of 500 ng/mL. After these treatments, the cells were counted and then washed twice with phosphate-buffered saline (PBS). After washing, the cells were suspended in 200 µL PBS and prepared on Mylar film (25 µm) using Cytospin, fixing with 100% ethanol and drying at room temperature.

Experimental Setup

The X-ray fluorescence (XRF) analysis was accomplished by 8-GeV Synchrotron radiations from the storage ring at a maximum current of 100 mA passing through a film monochromator. The beamline BL37XU was used, XRF imaging experiments was performed under vacuum, and spectra analysis was performed in the air. The incident X-ray energy was 14.3 keV, focused using a Kirkpatrick–Baez optical setup. The incident beam size was about 4×5 μm^2. The incident and transmitted photon fluxes was monitored with an ion chamber, and the fluorescent X-rays were collected by a solid-state detector (SSD) following procedures previously reported *(9–11)*.

XRF Imaging and Spectra

The XRF imaging technique was used to investigate the intracellular distribution of iron and other elements. X-Y step pulse motors moved the sample stage. The measurement areas were divided into matrices of 40×40 pixels. A single-channel analyzer was used to measure the fluorescence from iron at each pixel, with measurement times of 3 s per pixel. For quantitative analysis, the point spectra were measured with a multichannel analyzer at certain points in the samples. The measurement time was 200 s for each spectrum.

Chemical State Analyses Procedures

X-Ray absorption near-edge structure (XANES) spectroscopy is sensitive to the valence state and chemical environment of the absorbing elements. If the incident energy near the absorption edge is properly chosen, selective excitation of specific chemical species will occur. The XANES spectra of $Fe^{II}SO_4$ and $Fe_2^{III}(SO_4)_3$ were used as reference materials and are shown in the Results section. At energies near the absorption edge, such as 7.120 keV, Fe(II) is selectively excited while the excitation of Fe(III) is suppressed. Because fluorescent X-rays are emitted along with the excitation of the absorbing elements, XRF imaging that distinguishes the chemical state can be obtained because of the sensitivity of the X-ray absorption coefficient to the oxidation state of the element.

RESULTS

The XRF analyses were performed on the LAD2, treated with several reagents. The distribution of trace elements was analyzed in the samples by scanning them in vacuum using the SR microbeam. The scanning areas were 40×40 μm^2, and the resulting mapping data are shown in Fig 1. Six elements were mapped: potassium calcium phosphorus, Fe, Zn, and Cu. In this technique, the elemental counts are directly proportional to their quantities in the sample. In the cells used as controls, P, Ca, and Zn accumulated

AU: Pls spell out SR at first use.

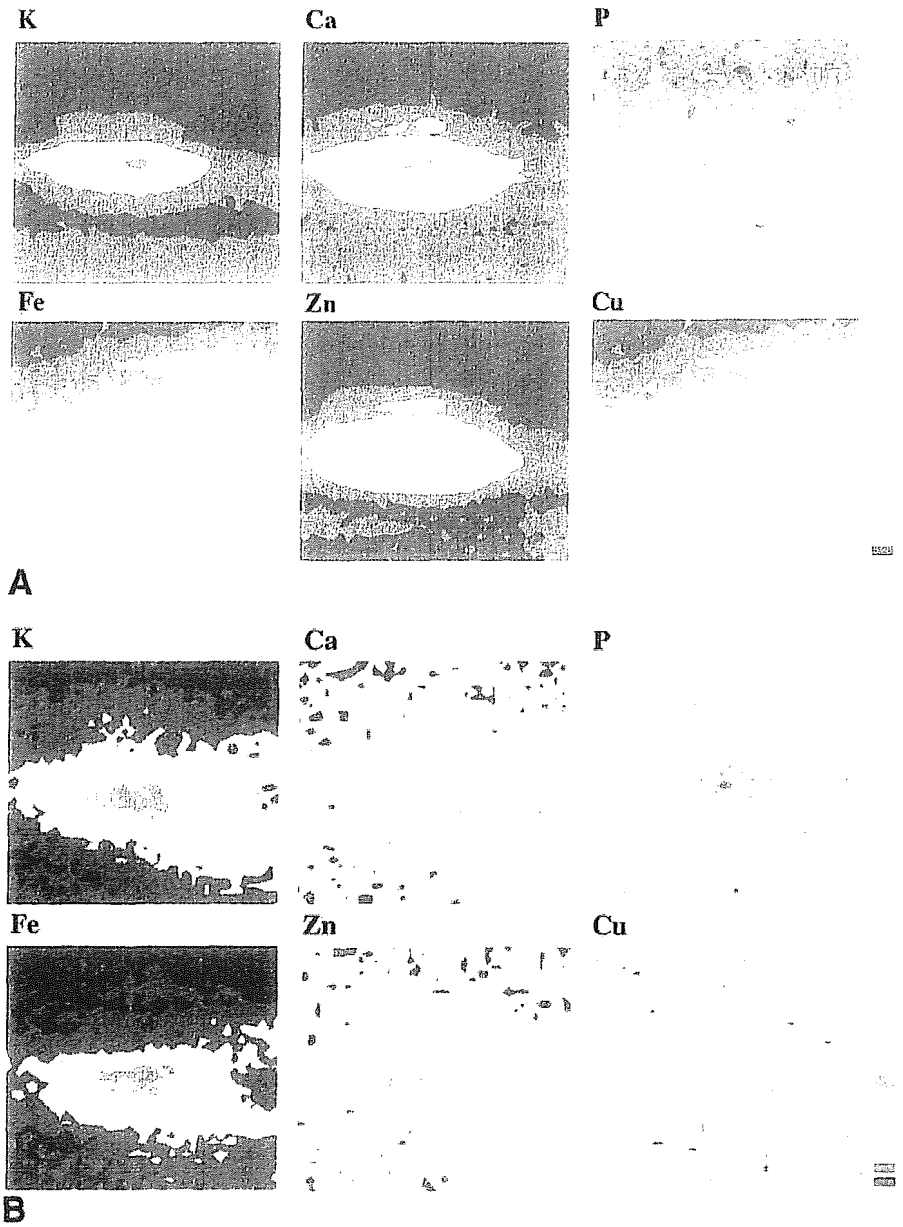

Fig. 1. Typical XRF imaging of LAD2. The figure represents elemental maps of Zn, Fe, K, Cu, Ca, and P. The scanning area was 40×40 μm^2. The image was obtained from LAD2 and cultured in medium for 30 min. **(A)** Control samples. The ranges of measured fluorescent intensities are from 0 to 1800 photons for Zn, from 20 to 260 photons for Fe, from 30 to 90 for Cu, from 0 to 2800 for K, from 0 to 700 for Ca, and from 20 to 100 for P. **(B)** IgE-mediated degranulation. The ranges of measured fluorescent intensities are from 50 to 160 photons for Zn, from 20 to 220 photons for Fe, from 20 to 70 for Cu, from 60 to 340 for K, from 30 to 130 for Ca, and from 10 to 60 for P. Each range is divided into eight levels. Each level has been assigned a shade of red, green, and blue, respectively.

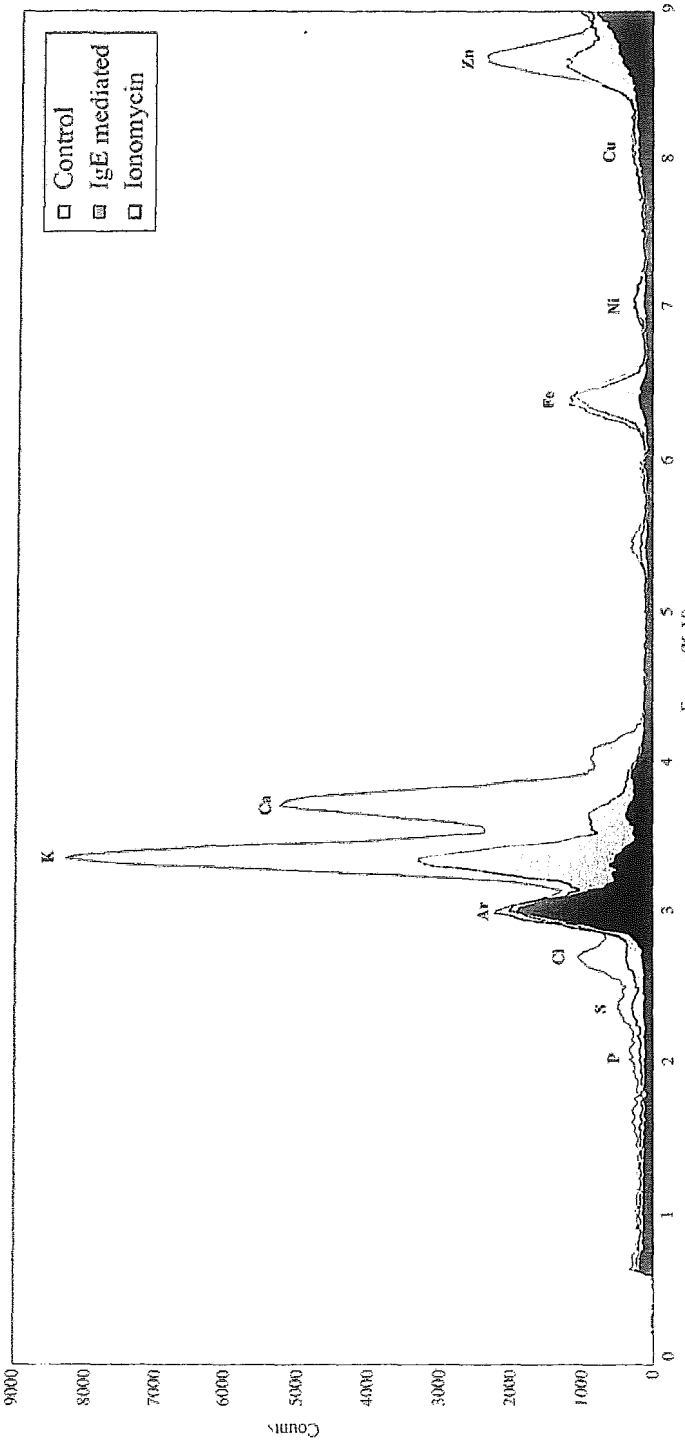

Fig. 2. Typical XRF spectra of LAD2: Control, sample, inducing IgE-mediated degranulation, and ionomycin stimulation. Measurement time was 200 s.

AU: Pls check degranulation